# Undulations of the potential-energy curves for highly excited electronic states in diatomic molecules related to the atomic orbital undulations

Alexandra Yiannopoulou and Gwang-Hi Jeung*
*Laboratoire Aimé Cotton, (Centre National de la Recherche Scientifique No. UPR3321), Bâtiment 506, and Applications Scientifiques du Calcul Intensif, (Centre National de la Recherche Scientifique No. UPR9029), Université de Paris–Sud, Bâtiment 505, 91405 Orsay, France*

Su Jin Park, Hyo Sug Lee, and Yoon Sup Lee
*Department of Chemistry and Center for Molecular Science, Korea Advanced Institute of Science and Technology, Taejon 305-701, South Korea*

(Received 13 July 1998; revised manuscript received 28 September 1998)

We present potential-energy curves for highly excited electronic states of diatomic molecules showing spectacular undulations including multiple barriers and wells. Those undulations unrelated to avoided crossings are closely correlated with the oscillations of atomic radial electron density in the Rydberg states. The LiHe, LiNe, and LiH cases are examined with an accurate quantum chemical calculation. For the $\Sigma^+$ states originating from the *ns*, *np*, *nd*, or *nf* states of lithium atom, $n-2$ potential barriers and the same number of potential wells exist. The $4\ ^1\Sigma_g^+(F)$ state of $Li_2$ also shows the energy barrier of the same origin. This spectroscopic property is supposed to be more general in diatomic molecules and other small molecules. [S1050-2947(99)08202-5]

PACS number(s): 31.25.−v, 31.50.+w, 34.20.−b

## I. INTRODUCTION

Laser absorption and fluorescence studies for the excited states of diatomic molecules often show complex potentials. Recent progress in cold atom trapping and photoassociation spectroscopy [1] has renewed the interest in long-range interatomic potentials [2–4]. The shape of the potential-energy curve at long range is important for the spectroscopic characterization of electronic states. For example, the existence of potential barriers for excited states having a shallow potential well in metal–rare-gas diatomic molecules has led to a revision of the ground and excited bond energies [5–7]. This barrier sometimes separates a significantly deep external potential well from a much deeper internal well [8]; it may accompany only a shallow external well [9] or the outer well may be barely observable [10]. The origin of those barriers, which are unrelated to avoided crossings caused by neutral-neutral (valence or Rydberg) or neutral ionic coupling, has been vaguely attributed to the repulsive interaction between the long-range electron density of the metal atom and the rare-gas-atom [5,6,8–10]. Our recent work on LiAr [11] has given a plausible explanation for one-Rydberg state $C\ ^2\Sigma^+$, where one barrier separates the major inner well from the outer shallow well. We speculated there that the undulations in the potential-energy curve would appear in the metal–rare-gas diatomic molecules in general and would be directly related to the atomic orbital oscillations. Were this true, higher Rydberg states should have two barriers separating two or three potential wells (depending upon the strength of the longest-distance van der Waals interaction) and still higher states should have three potential barriers separating three or four potential wells, etc.

We have performed highly accurate *ab initio* quantum chemical calculations for LiH, LiHe, and LiNe molecules to clearly check that assumption. The attractive interaction for the Rydberg states of those molecules is generally small and the amplitude of the undulations is even smaller. Subsequently, the method of calculation should be free of any approximation and the computation should be accurate enough. We have used an *ab initio* quantum chemical calculation, with a large-scale configuration interaction (CI). A large set of the atomic basis functions has been used to accurately describe a large number of the molecular electronic states. Our study reveals a clear correlation between the number of potential barriers and the number of the atomic orbital nodes. The undulation of the potential-energy curve does not seem to be restricted to the metal–rare-gas or the metal hydride diatomic molecules. We show an alkali dimer case in which a barrier of the same origin is apparent.

The presence of a single barrier for the highly excited electronic states has been observed or calculated before, a number of them being cited above [5–12]. Du [13] has shown a semiempirical calculation on a $^2\Sigma^+$ state of NaHe correlating with the $Na(8p)$ state, which has a wildly undulating potential-energy curve. Judging from the limited data available to us, that state seems to have four potential barriers with the outermost maximum at around 30 bohrs. Our work predicts one more barrier (see below). An effective core potential calculation by Boutalib and Gadéa for the electronic states of LiH [14] has also shown a single potential barrier and gave a correct explanation for that. Unfortunately, that work did not explore a long enough internuclear distance region. A recent work on the Ca-Xe collision by Isaacs and Morrison [15] has revealed a remarkable oscillatory behavior of the cross section as a function of the colli-

*Author to whom correspondence should be addressed. Electronic address: jeung@asci.fr

 

sion energy and as a function of the magnetic quantum number. The orbital alignment intervening in the collision process was supposed to be responsible for this astonishing behavior.

Our work does not claim any priority of observing the presence of a single potential barrier. We have just paid more attention to it from a quantum chemist's point of view. Then we have pushed the limit of the present state quantum chemical calculation to its extreme to reveal a general and systematic presence of the undulations including multiple potential barriers and wells in the potential-energy curves. We also give here a consistent explanation for such a spectroscopic property.

## II. METHOD OF CALCULATION

A large set of the atomic basis function has been used for the H, He, Li, and Ne atoms. First, each Gaussian atomic primitive function has been optimized to best describe the lowest electronic states of different symmetry ($^2S$, $^2P$, $^2D$, $^2F$, and $^1S$). For higher atomic states of those symmetries, additional diffuse Gaussian functions have been chosen in a geometric progression. For the high-angular-momentum ($l=2$ and 3 for H and $l=3$ and 4 for He and Ne) basis, the Gaussian exponents were obtained to minimize both the intra-atomic correlation (for hydrogen, the anion energy) and the interatomic polarization-correlation energies. This constitutes a long technical procedure and the resulting basis sets are reported in Table I. Our Hartree-Fock (HF) calculated atomic ground-state energies in hartrees are $-0.499\,71$ for H, $-2.861\,28$ for He, $-7.432\,57$ for Li, and $-128.540\,35$ for Ne, which are close to the HF limit energies [16] $-0.5$, $-2.861\,68$, $-7.432\,73$, and $-128.547\,10$, respectively. Our atomic ground-state energies calculated in the CI are $-78.959$ eV for He and $-203.344$ eV for Li, which are close to the experimental values [17] $-78.983$ and $-203.429$, respectively.

The ionization energies of the lithium atom obtained by a practically full CI calculation are reported in Table II. The energy differences between the atomic states are in good agreement with the experimental values. The energy difference between the $4d$ and $4f$ states is very small, the experimental result being only 7 $cm^{-1}$. Special care was taken in optimizing the $d$ and $f$ atomic basis functions (ABFs) to reproduce this small difference. The remaining errors in comparison to the experimental values may be compensated for in positioning the asymptotic energies for the molecular electronic energies when state-to-state spectroscopic data are needed. This does not affect the shape of each potential-energy curve (PEC) because the compensation just translates each PEC. Only the $\Sigma^+$ states made from the $4d$ and $4f$ states showed a slight change with the choice of basis set giving a different $4d$-$4f$ splitting (we have experimented with a trial basis set giving 44 instead of 7 $cm^{-1}$).

The calculated electron affinity of the hydrogen atom is 0.736 eV, which is close to the experimental value [18] of 0.756 eV (we do not know how accurate this experimental value is). A good description of the electron affinity is, however, crucial to obtain reliable PECs for the $^1\Sigma^+$ states of LiH. Indeed, our initial trial basis, which gave an electron affinity of 0.636 eV (803 $cm^{-1}$ smaller than our final basis), gave a potential energy of the $^1\Sigma^+$ symmetry significantly higher than our final basis for the ionic part. The largest energy decrease from our initial to our final hydrogen basis was 252 $cm^{-1}$ at $R=5$ bohrs for the ground state, 356 $cm^{-1}$ at 8 bohrs for the $2\ ^1\Sigma^+(A)$ state, 701 $cm^{-1}$ at 17 bohrs for

TABLE I. Atomic basis functions for Li, H, He, and Ne atoms: exponents for the Gaussian-type functions and the contraction coefficients (in parentheses).

| Atom | $l$ | Exponent (contraction coefficient) |
|---|---|---|
| Li | $s$ | 1938.0 (0.000 54), 291.5 (0.004 17), 66.53 (0.021 14), 19.00 (0.078 98), 6.305, 2.340, 0.9599, 0.4188, 0.091 61, 0.041 40, 0.019 41, 0.009 954, 0.005 105, 0.002 618, 0.001 342 |
| | $p$ | 9.745, 2.187, 0.6004, 0.1838, 0.066 25, 0.027 07, 0.011 25, 0.005 488, 0.002 677, 0.001 306 |
| | $d$ | 0.3913, 0.097 34, 0.033 06, 0.013 46, 0.005 679, 0.002 396 |
| | $f$ | 0.019, 0.0066, 0.0027 |
| H | $s$ | 19.79 (0.1196), 2.945 (0.084 82), 0.7209, 0.2301, 0.085 52, 0.019 |
| | $p$ | 2.7, 1.0, 0.31, 0.087 |
| | $d$ | 1.1, 0.19 |
| He | $s$ | 245.6 (0.002 45), 36.36 (0.1895), 8.137 (0.8978), 2.269, 0.7276, 0.2623, 0.096 37, 0.046 |
| | $p$ | 4.191, 1.27, 0.3848 |
| | $d$ | 3.742, 1.069 |
| Ne | $s$ | 20 170.0 (0.000 63), 3021.0 (0.004 92), 684.3 (0.2529), 194.0 (0.095 61), 64.45, 24.12, 9.628, 3.176, 1.397, 0.5774, 0.2459, 0.1230 |
| | $p$ | 67.27 (0.1222), 15.95 (0.7460), 5.119, 1.877, 0.7311, 0.2997, 0.1238, 0.090 17, 0.036 09 |
| | $d$ | 6.6, 2.2, 0.7333 |
| | $f$ | 4.578, 1.477 |

TABLE II. Ionization energies for the lithium atom (in $cm^{-1}$).

| State | Experiment | Calculation | Error |
|---|---|---|---|
| $Li^+$ | 0 | 0 | 0 |
| $5p$ | 4471 | 4464 | 7 |
| $5s$ | 5187 | 5185 | 2 |
| $4f$ | 6857 | 6847 | 10 |
| $4d$ | 6864 | 6854 | 10 |
| $4p$ | 7017 | 7009 | 8 |
| $4s$ | 8475 | 8471 | 4 |
| $3d$ | 12 204 | 12 200 | 4 |
| $3p$ | 12 562 | 12 543 | 19 |
| $3s$ | 16 281 | 16 271 | 10 |
| $2p$ | 28 583 | 28 525 | 58 |
| $2s$ | 43 487 | 43 441 | 46 |

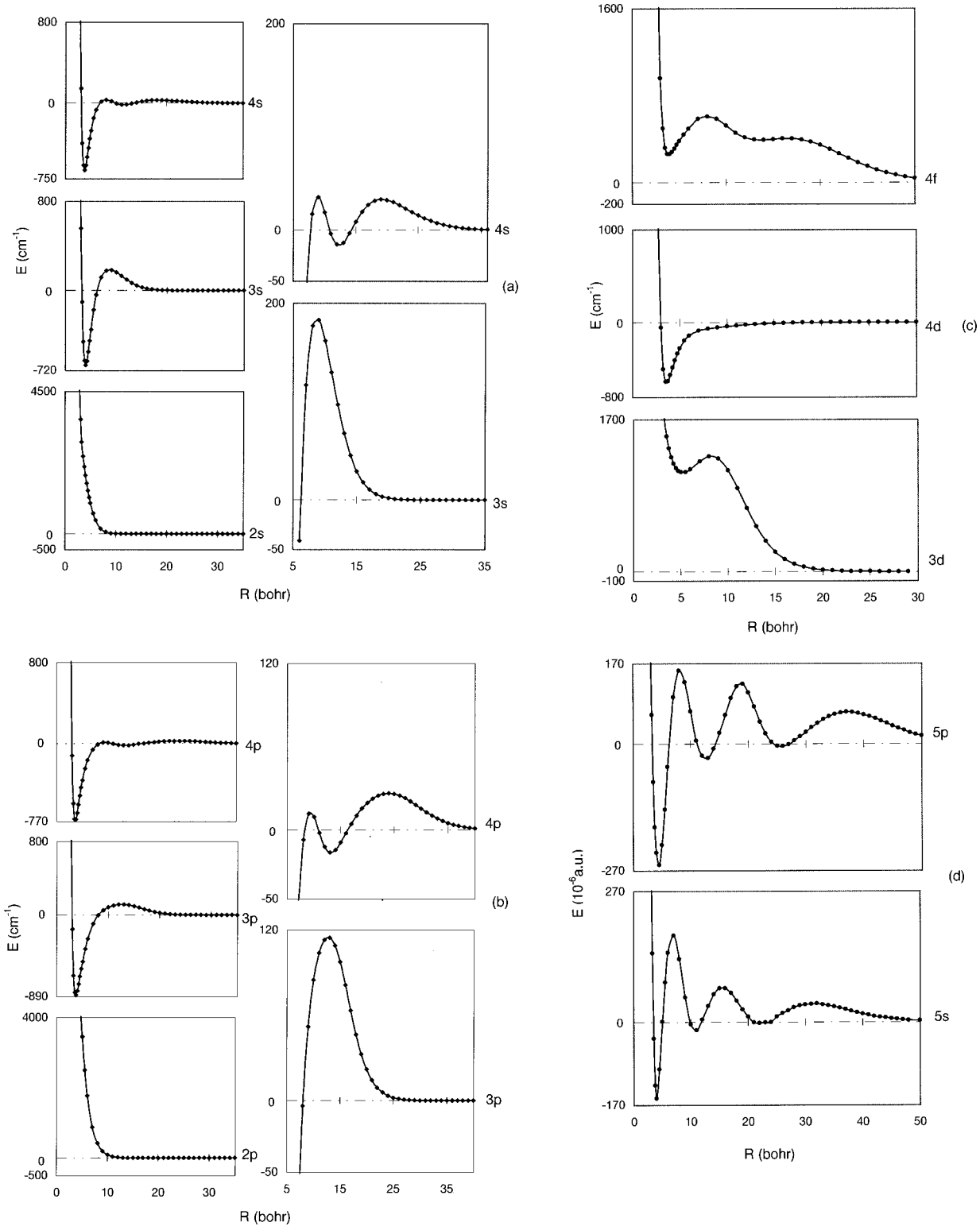


FIG. 1. (a)–(c) Potential-energy curves for the $^2\Sigma^+$ states of LiHe and (d) the valence electron potential curves for the $5s\ ^2\Sigma^+$ and $5p\ ^2\Sigma^+$ states of LiHe ($R$ in bohrs and $E$ in cm$^{-1}$).

the $3\ ^1\Sigma^+(C)$ state, and 720 cm$^{-1}$ at 28 bohrs for the $4\ ^1\Sigma^+(D)$ state. The energy decrease for the neutral part of the $^1\Sigma^+$ states and the $^3\Sigma^+$ states is insignificant. Our remaining error for the electron affinity (supposing that the above-mentioned experimental value is correct), 0.02 eV, can be compensated for by decreasing each potential energy by extrapolating (i.e., by adding about 20% of the above energy differences) for each $^1\Sigma^+$ state and each internuclear distance.

For molecular CI calculations, we have used the MOLCAS program package [19]. For LiH and LiHe, all electrons were allowed to occupy a large set of active space and then all possible single and double substitutions were done. This makes a full CI quality calculation. For LiNe, the $1s$ electron

pair of the Ne atom was frozen and the $2s$ and $2p$ electrons were allowed to make all possible single and double substitutions, while the Li electrons were all correlated. This makes a large-scale multireference CI (MRCI). The molecular-orbital basis was optimized by performing a multiconfiguration HF calculation, although the choice of the particular molecular orbital sets was proved not to affect the final CI energies in the LiH and LiHe cases. This is an indirect proof for the good convergence of the MRCI calculation. No virtual molecular orbital was excluded in the CI.

## III. RESULT AND DISCUSSION

### A. LiHe

The PECs for the $^2\Sigma^+$ states of the LiHe molecule, dissociating into the $2s$, $2p$, $3s$, $3p$, $3d$, $4s$, $4p$, $4d$, and $4f$ states of Li, are reported in Fig. 1. The $2s\Sigma^+$ and $2p\Sigma^+$ states are purely repulsive, the $3s\Sigma^+$ [Fig. 1(a)] and $3p\Sigma^+$ [Fig. 1(b)] states have one potential barrier, and the $4s\Sigma^+$ and $4p\Sigma^+$ states have two potential barriers and two potential wells. All those states show a very shallow van der Waals attraction at the outermost part of the PEC, which will not be discussed further in this work.

To understand the presence of potential barrier in those states, it is necessary to consider the corresponding atomic orbitals (AOs) or radial electron densities [see Fig. 2(a)]. The Rydberg *ns* or *np* states have the $n-2$ nodes in the valence region (not counting the single node of *ns* in the core region). When the compact He electron distribution makes contact with the diffuse Li electron distribution, the resulting interaction energy can be divided into the Coulomb repulsion (called the steric effect in chemistry), the charge-induced–dipole attraction, the exchange attraction, and the dispersive attraction according to the intermolecular (or interatomic) theory. Of course, all those effects are not strictly separable and it is difficult to predict the interaction energy at such internuclear distances ($R$) where the two-electron distribution functions overlap. The innermost principal potential well of the Rydberg states are due to the charge-induced–dipole attraction term. (Of course, our *ab initio* calculation includes all the nonrelativistic Hamiltonians and solves the Schrödinger equation practically exactly. The partition discussed above is only a conventional partitioning.)

Comparing Figs. 1 and 2, it is evident that the steric repulsion reproduces faithfully the atomic radial electron distribution of the lithium atom for $R$ sufficiently longer than the innermost well minimum. The number of potential barrier (one in $3s\Sigma^+$ and $3p\Sigma^+$, two in $4s\Sigma^+$ and $4p\Sigma^+$) coincides with the number of local density maxima in the valence region $(n-2)$. To check the correlation between the atomic density undulation and the molecular potential undulation, the electron density of the $4s\Sigma^+$ state of LiHe is shown in Fig. 3 as solid lines together with the atomic density of free Li as a dotted line. Here the natural molecular orbitals, which have nearly integer occupations [$1\sigma = 1.9936$ (Li, $1s^2$), $2\sigma = 1.9842$ (He, $1s^2$), and $3\sigma = 1.0000$], were used. The internuclear distance is 18 bohrs, which is close to the outermost top of the barrier distance (see Table III). The $1s^2$ densities of Li and He in the molecule cannot be distinguished from the free atomic densities. In contrast, the electron density of the Li($4s$) atomic orbital is slightly polarized ($3\sigma$) in the LiHe molecule. The main deformation is due to an orthogonalization effect (a peak at the He nucleus position). Otherwise, the molecular density is only slightly different from the sum of the atomic electron densities. This figure clearly shows that the helium nucleus is sitting just on top of the barrier density.

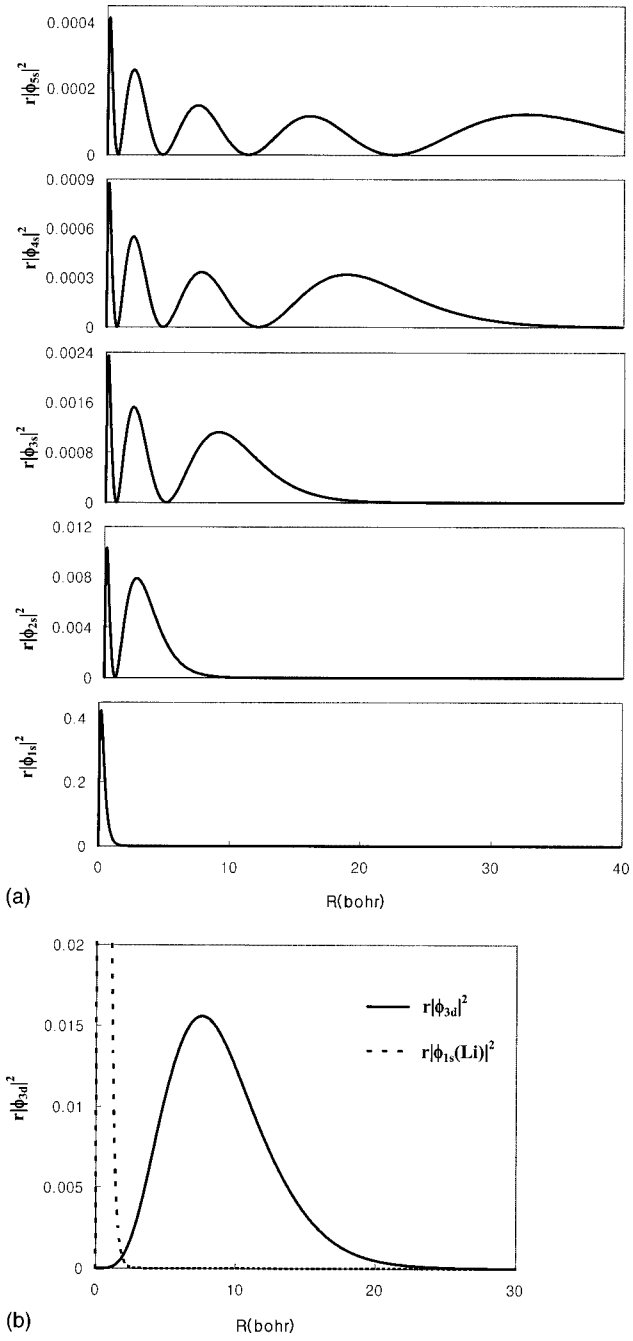


FIG. 2. Radial electron densities for the atomic states of the lithium ($R$ in bohrs): (a) the $1s^2$, $2s$, $3s$, $4s$, and $5s$ natural atomic orbitals and (b) the $1s^2$ (dotted line) and $3d$ (solid line) natural atomic orbitals.

The $3d\Sigma^+$ state shows a short-distance (around 5 bohrs) potential well [Fig. 1(c)]. The formation of this well has a slightly different origin from the main potential well of the $ns\Sigma^+$ or $np\Sigma^+$ states. Indeed, while the Rydberg electron densities in this region for the $ns\Sigma^+$ and $np\Sigma^+$ states are small but not negligible, the radial electron density of the $3d$

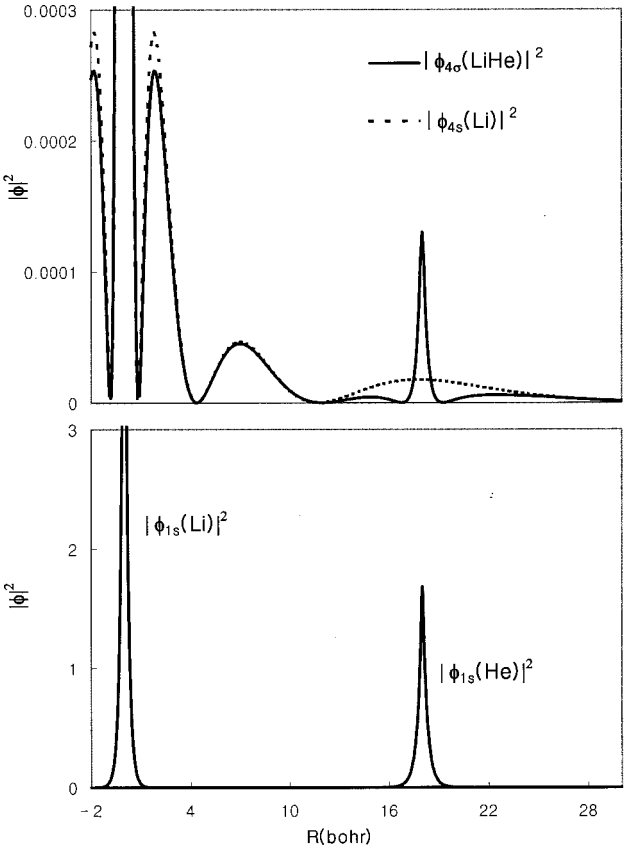


FIG. 3. Axial electron densities of the natural molecular orbitals for the $4s\ ^2\Sigma^+$ electronic state of LiHe at $R(\mathrm{Li\text{-}He}) = 18$ bohrs (near the largest $R_{\max}$). The Li atom is at $R = 0$ and the He atom is at $R = 18$ ($R$ in bohrs). The dotted line represents the electron density of the Li($4s$) natural atomic orbital.

AO tends to zero as $R$ becomes small [see Fig. 2(b)]. The steric repulsion becomes smaller while the charge-induced–dipole term becomes larger (the effective charge of Li tends to 1) at short $R$. The same applies to the $4d\Sigma^+$ state. The inner potential barrier of the $4d\Sigma^+$ state originates from the same situation, while the outer potential well is brought about by the steric interaction minimum coming from the nodal minimum of the $4d$ radial electron distribution and the helium electrons. In a way, the helium atom is playing the role of a differential detector of the lithium radial electron density.

We have drawn the valence electron PECs in Fig. 1(d), while Figs. 1(a)–1(c) show the total molecular PECs. The valence electron potential energy at each $R$ has been obtained by subtracting the total molecular energy of $\mathrm{LiHe}^+$ from that of the LiHe energy. So, as the highly excited Rydberg states of LiHe increasingly resemble the ground state of $\mathrm{LiHe}^+$, the valence electron PEC should tend to zero at all $R$. The numbers of potential barriers and potential wells in the valence electron PEC are the same as in the usual (total molecular) PECs. The valence electron potential is also called the valence electron diffusion potential.

Figure 1 also shows that the height of the potential barrier or the depth of the potential well becomes smaller in going from the lower to the higher states. This is in complete agreement with the fact that the atomic electron density of Li becomes smaller in going from the lower to the higher states (Fig. 2), resulting in a smaller steric effect for higher molecular states than in lower states. Subsequently, the amplitude of undulations in the PEC should gradually decrease for still higher states than presented in Fig. 1.

TABLE III. Minima and maxima of the potential-energy curves. Energies are with respect to the corresponding asymptotes.

| Molecule | Electronic state | $E_{\min}$ ($\mathrm{cm}^{-1}$) | $R_{\min}$ (bohrs) | $E_{\max}$ ($\mathrm{cm}^{-1}$) | $R_{\max}$ (bohrs) |
|---|---|---|---|---|---|
| LiHe | $3s\ ^2\Sigma^+$ | −681 | 3.98 | 184 | 8.65 |
| | $3p\ ^2\Sigma^+$ | −884 | 3.71 | 113 | 12.74 |
| | $3d\ ^2\Sigma^+$ | 1094 | 5.23 | 1283 | 8.20 |
| | $4s\ ^2\Sigma^+$ | −667 | 3.72 | 31 | 7.91 |
| | | −15 | 11.29 | 30 | 18.2 |
| | $4p\ ^2\Sigma^+$ | −766 | 3.62 | 16 | 9.49 |
| | | −16 | 13.18 | 27 | 23.60 |
| | $4d\ ^2\Sigma^+$ | −645 | 3.60 | 5 | 30.5 |
| | $4f\ ^2\Sigma^+$ | 260 | 3.91 | 608 | 8.09 |
| | $5s\ ^2\Sigma^+$ | −650 | 3.65 | −7 | 8.12 |
| | | −15 | 10.19 | 13 | 15.73 |
| | | −1 | 22.04 | 8 | 31.48 |
| | $5p\ ^2\Sigma^+$ | −659 | 3.65 | 7 | 8.92 |
| | | −12 | 12.33 | 27 | 18.76 |
| | | −2 | 25.44 | 15 | 37.51 |
| LiNe | $3s\ ^2\Sigma^+$ | −433 | 4.13 | 107 | 9.12 |
| | $3p\ ^2\Sigma^+$ | −567 | 3.83 | 90 | 12.39 |
| | $3d\ ^2\Sigma^+$ | 518 | 4.57 | 821 | 8.15 |
| | $4s\ ^2\Sigma^+$ | −729 | 3.93 | 4 | 9.1 |
| | | −4 | 11.6 | 17 | 18.3 |
| | $4p\ ^2\Sigma^+$ | −754 | 3.85 | 12 | 11.2 |
| | | 3 | 14.6 | 22 | 22.9 |
| LiH | $3s\ ^3\Sigma^+$ | −2050 | 4.12 | 249 | 9.05 |
| | $3p\ ^3\Sigma^+$ | −2005 | 4.13 | 128 | 13.66 |
| | $3d\ ^3\Sigma^+$ | 1284 | 5.16 | 1879 | 8.94 |
| | $4s\ ^3\Sigma^+$ | −1423 | 4.04 | 2 | 8.35 |
| | | −55 | 10.92 | 44 | 18.27 |
| | $4p\ ^3\Sigma^+$ | −1453 | 4.12 | −55 | 8.95 |
| | | −85 | 12.42 | 31 | 25.0 |
| | $4d\ ^3\Sigma^+$ | −1143 | 4.15 | 10 | 28.40 |
| | $4f\ ^3\Sigma^+$ | 53 | 4.48 | 868 | 8.86 |
| | $5s\ ^3\Sigma^+$ | −1243 | 4.06 | −55 | 8.9 |
| | | −56 | 9.6 | 18 | 16.0 |
| | | −4 | 21.9 | 11 | 31.8 |
| | $5p\ ^3\Sigma^+$ | −1282 | 4.11 | −70 | 9.0 |
| | | −80 | 9.7 | 13 | 19.8 |
| | | 3 | 24.0 | 20 | 41.5 |

### B. LiNe

The same features are present in the LiNe molecule (Fig. 4) as in the LiHe case. Although the neon atom contains eight more electrons than the helium atom, the size of the valence electron distribution is about the same: The mean expectation values for the electron radius $\langle r \rangle$ are 1 bohr for H, 0.927 bohr for He, 3.874 bohrs for the $2s$ AO of Li, and 0.965 bohr for the $2p^6$ AO of Ne [16]. The level of calcula-

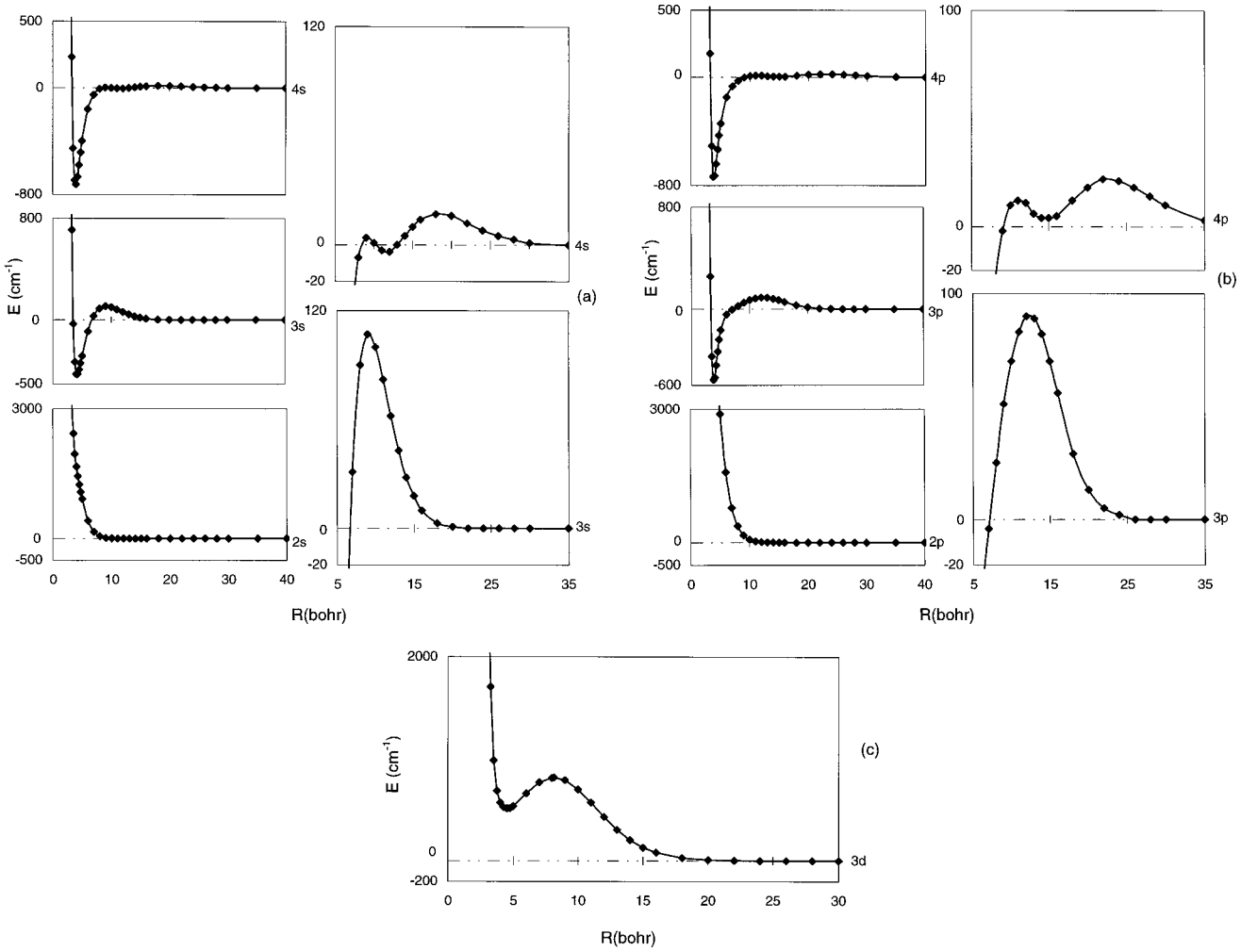


FIG. 4. Potential-energy curves for the $^2\Sigma^+$ electronic states of LiNe ($R$ in bohrs and $E$ in cm$^{-1}$).

tion for the LiNe molecule should not be as accurate as in the LiHe case because the $1s^2$ core electrons are not correlated and the $2s^22p^6$ electrons are only partially correlated. It is difficult to measure the error resulting from this neglect. However, we think that the undulations for LiNe shown in Fig. 3 should be considered correct as the whole picture is consistent with the LiHe case. The locations of the potential barriers ($R_{\max}$) and the potential wells ($R_{\min}$) for both the LiHe and LiNe cases are numerically close too.

### C. LiH

We expect a different interaction scheme for the LiH case. This is a case where both atoms have an unpaired electron, so the electron spin pairing effect could be regarded as a dominant effect. Our calculated PECs for the $^3\Sigma^+$ states are reported in Figs. 5(a)–5(c). The Pauli principle imposes a repulsion between the two valence electrons in the triplet states. This results in a strong correlation between the atomic orbital distributions of the lithium Rydberg states and the corresponding molecular potential undulation. This is indeed nicely reproduced in Figs. 5(a)–5(c).

The $^1\Sigma^+$ case of the LiH molecule is more complicated than the $^3\Sigma^+$ case because this symmetry includes not only the neutral configurations $Li^0H^0$ but also the ionic configurations $Li^+H^-$. This results in a series of neutral-ionic diabatic couplings involving all the $^1\Sigma^+$ electronic states from $2s+1s$ to $4f+1s$ (the ionic asymptote $Li^++H^-$ should lie approximately 759 cm$^{-1}$ higher than the $4f+1s$ state and 911 cm$^{-1}$ lower than the $5s+1s$ state if the electron affinity of Ref. [18], 0.756 eV, is correct). Also present are the neutral-neutral avoided crossings. As a detailed discussion of the spectroscopic aspects for the $^1\Sigma^+$ states requires a lot of space, it will be discussed elsewhere. Nevertheless, the undulating nature of the PECs exists for the $^1\Sigma^+$ state too. We show in Fig. 5(e) the $^1\Sigma^+$ states derived from the $4s$ and $4p$ atomic states of Li where the ionic-neutral diabatic coupling occurs at long $R$ in a very localized way (not shown in this figure). The potential barriers and potential wells are situated in slightly different internuclear distances; the barrier heights and well depths are different from the $^3\Sigma^+$ case. This results from the usually observed singlet-triplet energy differences (at large $R$, this difference comes mainly from the exchange integral).

The $\Sigma^+$ states correlated with the $5s$ and $5p$ atomic orbitals show three potential barriers. The innermost one appears as a slight bump on the attractive part of the curve. The effective charge experienced by the hydrogen atom at this distance is large (close to one), as it is approximately equal to the nuclear charge (3) minus the integrated Li atomic electron density up to this distance in the spherical coordinates

centered at the lithium nucleus. This may explain the small innermost bump on the attractive side in the PECs for the $5s$ and $5p\ ^3\Sigma^+$ states. The difference PECs, subtracting the PEC of the ground state of $LiH^+$ from the $5s$ and $5p\ ^3\Sigma^+$ PECs of LiH, are reported in Fig. 5(d). This figure shows the undulations of Fig. 1(d). The $4f\ ^3\Sigma^+$ state shows an uneven potential-energy decrease for long distance apart from the main barrier around 4 bohrs [Fig. 5(c)]. The origin of this further complication, which is very similar to the LiHe case [Fig. 1(c)], is unclear.

The barrier heights, the well depths, and their positions ($R_{\min}$ and $R_{\max}$) for LiH, LiHe, and LiNe are summarized in Table III. The vibrational energy levels bound in the secondary and tertiary wells in most cases could not be calculated because those are high vibrational states and the vibrational equation with a multiple minimum-maximum potential-energy curve is difficult to solve. The spectroscopic constants for the ground state of $LiHe^+$ and $LiH^+$, for which no reliable experimental data were available, have been calculated. The result for the $LiHe^+$ is $R_e = 3.601$ bohrs, $D_e$

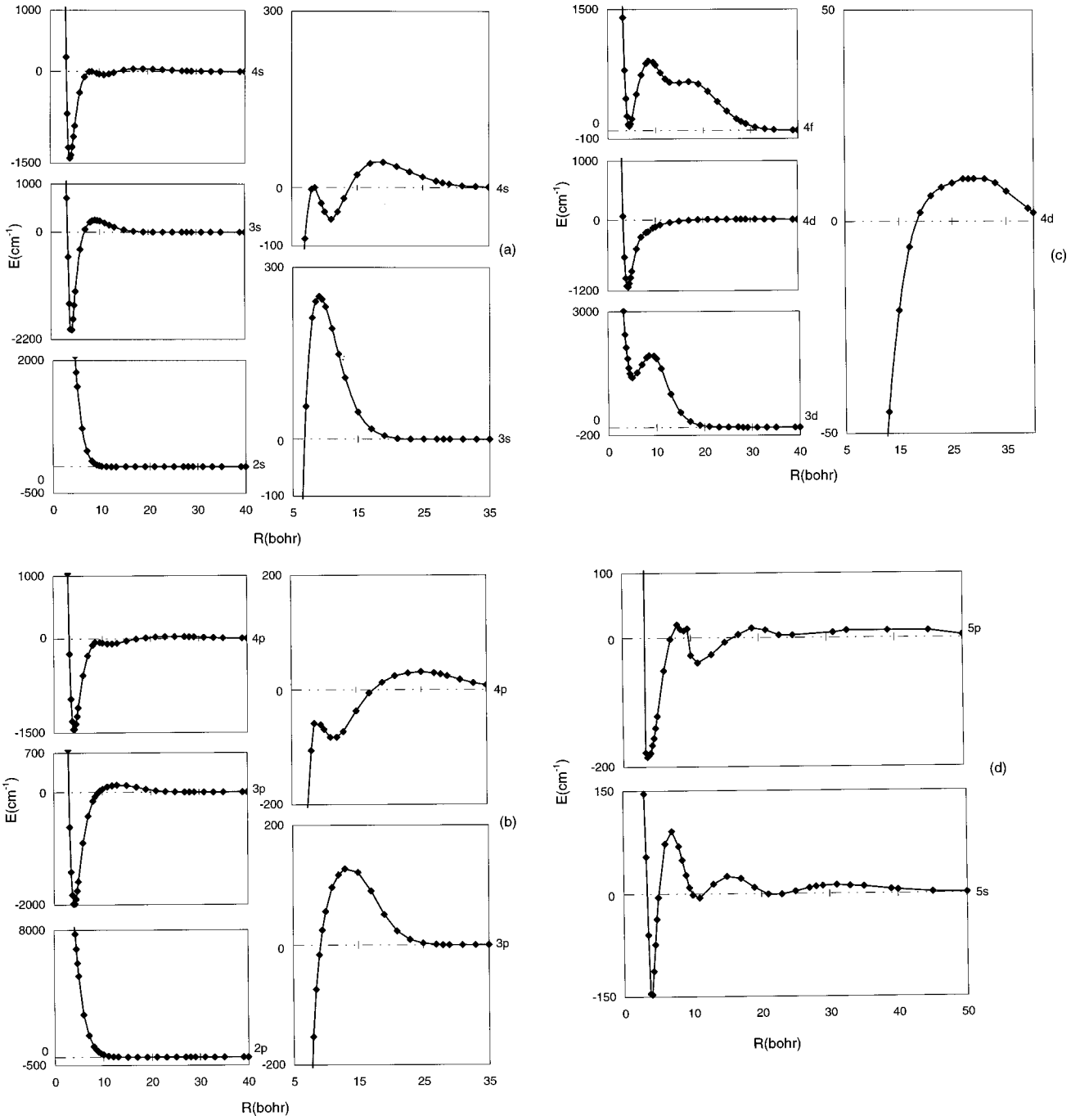


FIG. 5. Potential-energy curves for the (a)–(c) $^3\Sigma^+$ and (e) $^1\Sigma^+$ electronic states of LiH and the diffusion potential-energy curves for the least bound electron in the $5s$ and $5p\ ^3\Sigma^+$ states of LiH ($R$ in bohrs and $E$ in $cm^{-1}$).

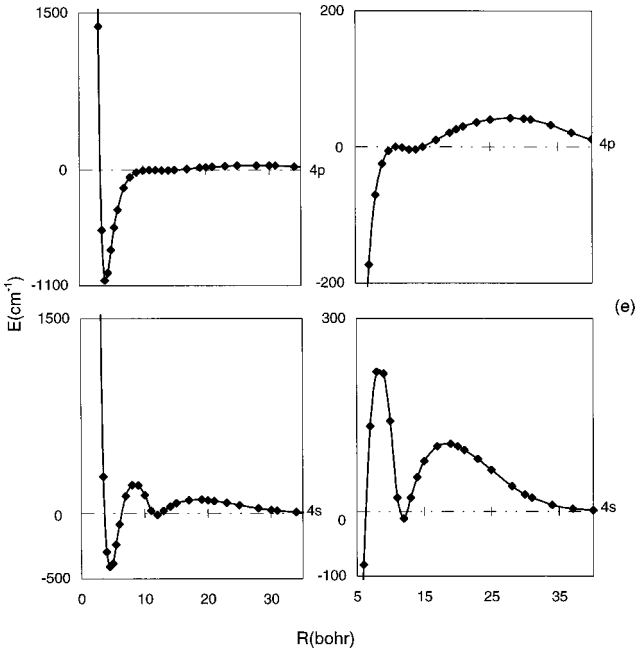


FIG. 5 (*Continued*).

$=630\,\mathrm{cm}^{-1}$, $\omega_e=275\,\mathrm{cm}^{-1}$, and $B_e=1.822\,\mathrm{cm}^{-1}$ for the reduced mass of 4645.84 a.u. ($^7$Li$^4$He). The result for $LiH^+$ is $R_e=4.284$ bohrs, $D_e=1145\,\mathrm{cm}^{-1}$, $\omega_e=494\,\mathrm{cm}^{-1}$, and $B_e=3.924\,\mathrm{cm}^{-1}$ for the reduced mass of 1606.4 a.u. ($^7$LiH). As the principal quantum number increases, the spectroscopic constants of the Rydberg states of LiHe and LiH approach those of the ground states of $LiHe^+$ and $LiH^+$, respectively. The $4d\ ^2\Sigma^+$ state of LiHe and the $4d\ ^3\Sigma^+$ state of LiH are already very close to the ground state of the corresponding cations.

### D. $Li_2$

The $3-5\ ^1\Sigma_g^+$ states of the lithium dimer are closely coupled states between the $3s+2s$ and $2p+2p$ neutral characters and $Li^+Li^-$ ionic character. This brings about oscillating transition dipole moments as functions of $R$ and induces predissociation. The predissociation of the $4\ ^1\Sigma_g^+(F)$ state has been studied recently by optical-optical double resonance excitation spectroscopy and by *ab initio* calculation [20]. This state, which is of neutral character, $3s+2s$ for $R\approx 16$ bohrs, acquires a partially ionic nature $Li^+Li^-$ for $18\leqslant R\leqslant 26$. The diabatic PECs for this region and the observed vibrational energy levels are reported in Fig. 6. As the diabatic coupling is small but non-negligible, neither the purely adiabatic scheme nor the diabatic scheme alone can be applied in this case, as can be deduced from the observed partial predissociation. It is not evident if $3s+2s$ at long distances shows a potential barrier as the (avoided) crossing blurs the purely neutral picture. However, the energy level of the shelf (plateaulike portion of the PEC) may give a clue to an answer to this question. Indeed, this shelf part, where the nature of the wave function is essentially $3s+2s$ before being contaminated by the ionic nature, is found to be lying above the $3s+2s$ asymptote both by analyzing the experimental spectra and by *ab initio* calculation. The experimental data gave the first observed predissociated energy level $v=33$, $J=13$, being 242.4 $\mathrm{cm}^{-1}$ higher than for the $3s+2s$ asymptote. The *ab initio* calculation gave the highest point of this long barrier (shelf), being 300 $\mathrm{cm}^{-1}$ higher than for the $3s+2s$ asymptote.

*Ab initio* calculations for the $^1\Sigma^+$ states of other alkali dimers have often shown the shelf portion of the PEC to be lying higher than the corresponding neutral asymptote, as can be seen in the examples of $Na_2$ [21] and $K_2$ [22]. On the other hand, high-lying Rydberg states of $\Sigma^+$ symmetry have often shown potential undulations that could not be connected to any avoided crossing. The origin of those spectroscopic features, which, to our knowledge, have not been analyzed before, as puzzling as they were, may be found also in the superposition of AO undulations.

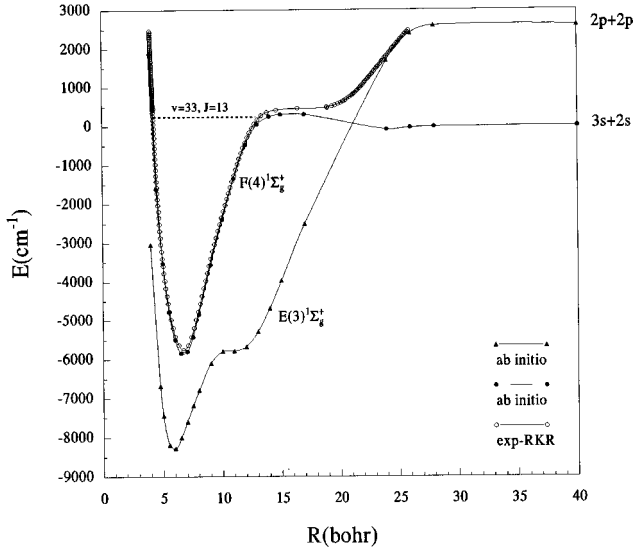


FIG. 6. Experimental Rydberg-Klein-Rees (RKR) curve for the $4(F)\ ^1\Sigma_g^+$ state and *ab initio* diabatic potential-energy curves for the $3(E)$ and $4(F)\ ^1\Sigma_g^+$ states of $Li_2$ ($R$ in bohrs and $E$ in $\mathrm{cm}^{-1}$).

## IV. CONCLUSION

The undulating PECs for the alkali-metal–rare-gas diatomic molecules remain to be experimentally checked, in particular, for the multiple barrier cases (the single barrier having been reported in many cases). The experimental observation for the alkali-metal–rare-gas case by the conventional laser (pump-dump) probe technique is not easy because the ground state is practically repulsive. Two conditions are necessary to observe high-lying Rydberg states: The ground potential well should be sufficiently deep and an intermediate state with vibrational functions overlapping well with the ground-state vibrational wave function should exist. A recently developed photoassociation technique for cold atoms may be more suited for this purpose. This technique approaches the excited state from the long-distance part instead of conventional laser spectroscopy where the short-distance part of the excited states is accessible. For the alkali hydride case, the condition for experimental observation is more favorable as the ground state has a deep potential well covering a wide range of $R$ and the $A$ state (covering a longer range of $R$) can be used as an intermediate state. We are aware of two experimental works on

LiH in progress, which may check this undulating property in the future.

We can extend this undulating property to polyatomic molecules, for example, $MX_n$ cases (where $M$ is a metal atom and $X$ is a rare-gas atom). That may reveal a three-dimensional (3D) structure in the potential-energy hypersurfaces related to the 3D electron distribution of the metal AO. This would result in multiple 3D geometrical local minima.

We wonder at this point if the undulations in the PECs for the Rydberg states of diatomics occur more generally. Sufficiently complete experimental data for those states are unfortunately rare. *Ab initio* calculation for the Rydberg states in other diatomic molecules requires a large amount of computational resources, so its realization is difficult for the time being. We have found a potential barrier for the Li($3s$) $+H_2$ collinear collision with a height of less than 100 $cm^{-1}$ when the $R$(H-H) distance was fixed at the equilibrium distance for the hydrogen molecule. This barrier diminishes greatly when the $R$(H-H) was allowed to relax [23], a degree of freedom that diatomic molecules do not have.

Traditionally, the interaction theory for two atoms has treated the steric repulsion term as a monotonically decaying single exponential [24] or polynomial [25] term. This was considered enough because most of the problem concerned the ground or low-lying electronic states. As higher and higher states and the long-distance part are being studied these days (see, for instance, Ref. [26] for the long-range interaction in the alkali dimers, Ref. [27] for the long-range interaction among H, He, and Li, and Ref. [28] for the long-range exchange interaction), a way to reflect the undulation originating from the overlap of two atomic radial densities should be appropriately taken into account in the light of our work. Let us emphasize here that all the nonrelativistic Hamiltonian terms were included (short- and long-distance interaction terms or whatever one might call the Hamiltonian in any partition scheme) in the *ab initio* method employed in this work. Our calculations are practically an exact treatment for the LiH and LiHe molecules.

Our extensive calculation about the potential-energy barrier for the Le($3s$) $+H_2$ collision revealed the lowest potential barrier height of 142 $cm^{-1}$ for a $C_{2v}$ approach. The barrier height monotonically increases as the collional geometry passes from the $C_{2v}$ approach to the $C_s$ approaches, then to the collinear ($C_{\infty v}$) approach. The lowest barrier height for the collinear approach is 308 $cm^{-1}$. The existence of the collision potential undulations including the activation barrier should be taken into account in the reactive collision process between an excited metal atom and diatomic molecules.

## ACKNOWLEDGMENTS

We would like to thank the Centre National de la Recherche Scientifique (CNRS) and the Korea Science and Engineering Foundation (KOSEF) for granting us a bilateral cooperation fund. A.Y. thanks the CNRS for financial support at the Applications Scientifiques du Calcul Intensif (ASCI) and the European Commission for financial support at the Laboratoire Aimé Cotton. This work has been communicated (RC03) in the 53rd OSU International Symposium on Molecular Spectroscopy, Columbus, Ohio.

[1] H. R. Thorsheim, J. Weiner, and P. S. Julienne, Phys. Rev. Lett. **58**, 2420 (1987).
[2] P. D. Lett, P. S. Julienne, and W. D. Phillips, Annu. Rev. Phys. Chem. **46**, 423 (1995), and references therein.
[3] H. Wang, X. T. Wang, P. L. Gould, and W. C. Stwalley, Phys. Rev. A **53**, R1216 (1996).
[4] A. Fioretti, D. Comparat, A. Crubellier, O. Dulieu, F. Masnou-Seeuws, and P. Pillet, Phys. Rev. Lett. **80**, 4402 (1998).
[5] P. A. Hackett, W. J. Balfour, A. M. James, W. M. Fawzy, B. J. Shetty, and B. Simard, J. Chem. Phys. **99**, 4300 (1993).
[6] W. H. Breckenridge, C. Jouvet, and B. Soep, in *Advances in Metal and Semiconductor Clusters*, edited by M. A. Duncan (JAI, Greenwich, 1995), Vol. 3, pp. 1–83, and references therein.
[7] A. Stangassinger, A. M. Knight, and M. A. Duncan, in Proceedings of the 53rd OSU International Symposium on Molecular Spectroscopy, Columbus, OH, 1998, p. 186.
[8] M.-C. Duval, O. Benoist d'Azy, W. H. Breckenridge, C. Jouvet, and B. Soep, J. Chem. Phys. **85**, 6324 (1986).
[9] S. J. Park, M. C. Kim, Y. S. Lee, and G.-H. Jeung, J. Chem. Phys. **107**, 2481 (1997).
[10] E. Hwang, Y.-L. Huang, P. J. Dagdigian, and M. H. Alexander, J. Chem. Phys. **98**, 8484 (1993).
[11] S. J. Park, Y. S. Lee, and G.-H. Jeung, Chem. Phys. Lett. **277**, 208 (1997).
[12] N. Y. Du and C. H. Greene, Phys. Rev. A **36**, 971 (1987).
[13] N. Y. Du (private communication).
[14] A. Boutalib and F. X. Gadéa, J. Chem. Phys. **97**, 1144 (1992).
[15] W. A. Isaacs and M. A. Morrison, Phys. Rev. A **57**, R9 (1998).
[16] C. Froese-Fischer, *The Hartree-Fock Method for Atoms* (Wiley, New York, 1977).
[17] C. E. Moore, *Atomic Energy Levels*, Natl. Bur. Stand. (U.S.) Cir. No. 467 (U.S. GPO, Washington, DC, 1971), Vol. 1.
[18] C. L. Peckeris, Phys. Rev. **126**, 1470 (1962).
[19] Version 4: K. Andersson, M. R. A. Blomberg, M. P. Fülscher, G. Karlström, R. Lindh, P.-Å. Malmqvist, P. Neogrády, J. Olsen, B. O. Roos, A. J. Sadlej, M. Schütz, L. Seijo, L. Serrano-Andrés, P. E. M. Siegbahn, and P.-O. Widmark, Lund University, Sweden, 1997.
[20] S. Antonova, G. Lazarov, K. Urbanski, A. M. Lyyra, L. Li, G.-H. Jeung, and W. C. Stwalley (unpublished).
[21] G.-H. Jeung, Phys. Rev. A **35**, 26 (1987).
[22] G.-H. Jeung and A. J. Ross, J. Phys. B **21**, 1473 (1988).
[23] H. S. Lee, Y. S. Lee, and G.-H. Jeung (unpublished).
[24] P. M. Morse, Phys. Rev. **34**, 57 (1929).
[25] J. W. Linett, Trans. Faraday Soc. **36**, 1123 (1940).
[26] M. Marinescu and A. Dalgarno, Phys. Rev. A **52**, 311 (1995).
[27] Z.-C. Yan, J. F. Babb, A. Dalgarno, and G. W. F. Drake, Phys. Rev. A **54**, 2824 (1996).
[28] G. Hadinger, G. Hadinger, O. Bouty, and M. Aubert-Frécon, Phys. Rev. A **50**, 1927 (1994).